



Enhanced glass forming ability of Fe-based amorphous alloys with minor Cu addition



Weiming Yang^{a,b,*}, Haishun Liu^{a,**}, Xingdu Fan^c, Lin Xue^{b,c}, Chaochao Dun^d, Baolong Shen^c

^a State Key Laboratory for Geomechanics and Deep Underground Engineering, School of Mechanics and Civil Engineering, School of Sciences, China University of Mining and Technology, Xuzhou 221116, People's Republic of China

^b Key Laboratory of Magnetic Materials and Devices, Ningbo Institute of Materials Technology & Engineering, Chinese Academy of Sciences, Ningbo 315201, People's Republic of China

^c School of Materials Science and Engineering, Southeast University, Nanjing 211189, People's Republic of China

^d Department of Physics, Wake Forest University, Winston Salem, NC 27109, USA

ARTICLE INFO

Article history:

Received 21 January 2015

Received in revised form 22 March 2015

Accepted 30 March 2015

Available online 6 April 2015

Keywords:

Fe-based amorphous alloys;
High saturation magnetization;
Glass-forming ability

ABSTRACT

A novel approach was reported that allows us to enhance glass-forming ability (GFA) of Fe-based amorphous alloys with high saturation magnetization by minor substitution Cu, which has a large positive heat of mixing and similar atomic radius with the main constituent Fe. The minor Cu substitution (<1 at.%) can substantially increase the GFA of Fe-based amorphous alloys with the primary phase that is not α -Fe (110) type phase. Using this strategy, Fe-based amorphous alloys with both high saturation magnetization and good GFA were developed. Our results reveal that the formation of competing crystalline phases is beneficial for the GFA. We anticipate that this work may guide the way for designing new Fe-based amorphous alloys with high saturation magnetization and large GFA concurrently.

© 2015 Elsevier B.V. All rights reserved.

1. Introduction

Owing to the combination of high saturation magnetization, high permeability, and the low cost of manufacture [1], the high Fe content amorphous alloys, especially at.% of Fe > 83% [2,3], have attracted great research interests ever since their first synthesis. They are inherently strong and have promising applications in toroidal cores, choke coils, power transformers, etc. [4]. Unfortunately, most of them were limited to thin ribbons with thickness less than 15 μm , since the critical cooling rate that required to hinder the crystallization of these alloys was generally larger than order of 10^5 – 10^6 K/s [5]. Actually, the synthesis of Fe-based amorphous alloys with high glass-forming ability (GFA) has always been one of the most important scientific interests [6–9]. The widely used strategy to couple the attractive properties of Fe-based amorphous alloys with good GFA is introducing multiple metallic or metalloid elements with negative heat of mixing and/or a prominent atomic size mismatch with the main constituent Fe [10–12]. However, the reduction of Fe inevitably leads to the deterioration of magnetic properties, especially the saturation magnetization [8,13,14]. Therefore,

it poses a serious challenge to develop Fe-based amorphous alloys with high saturation magnetization and good GFA concurrently.

In this paper, we report a novel approach that allows us to enhance GFA of high Fe content amorphous alloys by minor substitution of Cu, which has a large positive heat of mixing (+13 kJ/mol) [15] and similar atomic radius (0.124 nm) [16] with the main constituent Fe. Using this systematic approach, we can develop Fe-based amorphous alloys containing high iron content without deteriorating their good GFA and magnetic performance. Our approach reveals that the formation of competing crystalline phases is beneficial for the GFA, and might provide guidance to design new Fe-based amorphous alloys with high saturation magnetization and large GFA concurrently.

2. Experiments

Fe-based alloys ingots with nominal composition of $\text{Fe}_{72-x}\text{B}_{19.2}\text{Si}_{4.8}\text{Nb}_4\text{Cu}_x$ ($x = 0, 0.1, 0.2, 0.3, 0.4, 0.6, 0.8, 1.0$), $\text{Fe}_{84-x}\text{Nb}_2\text{B}_{14}\text{Cu}_x$ ($x = 0.0, 0.5, 1.0$ and 1.5) and $\text{Fe}_{86-x}\text{B}_7\text{C}_7\text{Cu}_x$ ($x = 0.0, 0.5, 0.7$ and 1.0) were prepared by arc-melting a mixture of pure Fe (99.99%), Nb (99.99%), B (99.5%), Si (99.999%), Cu (99.99%) and pre-alloyed Fe–C alloy in a highly purified argon atmosphere. The alloy ribbons and cylindrical rods were produced by single-roller using melt spinning method and copper mold casting method, respectively. The crystallization temperature (T_x) of as-quenched ribbons was measured by differential scanning calorimetry (DSC, NETZSCH 404C) with a heating rate of 0.67 K/s. Crystallization treatment was carried out by treating the as-quenched amorphous specimens at different temperatures under

* Correspondence to: W. Yang, State Key Laboratory for Geomechanics and Deep Underground Engineering, School of Mechanics and Civil Engineering, School of Sciences, China University of Mining and Technology, Xuzhou 221116, People's Republic of China.

** Corresponding author.

E-mail addresses: wmyang@cumt.edu.cn (W. Yang), liuhaishun@126.com (H. Liu).

vacuum followed by water quenching. Microstructure was examined by X-ray diffraction (XRD, Bruker D8 Advance) with Cu $K\alpha$ radiation.

3. Results and discussion

Fig. 1 shows the effects of Cu substitution on the crystallization behavior in $\text{Fe}_{72-x}\text{B}_{19.2}\text{Si}_{4.8}\text{Nb}_4\text{Cu}_x$ ($x = 0, 0.1, 0.2, 0.3, 0.4, 0.6, 0.8, 1.0$) alloys. The small Cu-addition yields two clearly separated peaks that assign to the first crystallization peaks T_{x1} and T_{x2} . The separation between the two peaks is practically insensitive to the further increase of the Cu content beyond a small, critical concentration ~ 0.3 at.%, as displayed in Fig. 1(a). It is known that the primary phase of the Cu-free glassy alloy is Fe_{23}B_6 phase. Although the first crystallization peak was the same from $x = 0.0$ to $x = 0.3$, as shown in Fig. 1(b), the primary phase changed into a mixture of Fe_{23}B_6 and bcc-Fe phases by increasing Cu content from $x = 0.1$ to 0.3, as shown in Fig. 1(c). However, from Fig. 1(d), the diffraction peaks of $x = 0.4$ alloy annealed for 600 s at 900 K correspond exclusively to the bcc-Fe phase. Therefore, the Cu-addition yields two separated the first crystallization peaks corresponding to the primary crystallization of bcc-Fe at T_{x1} and, subsequently, to the precipitation of Fe_{23}B_6 compounds at T_{x2} . The decrease of the onset temperature for the first crystallization stage reflects that the Cu substitution apparently lowers the configurational energy of the subcritical nucleus.

Based on the present and previous results [17], the effect of Cu on the process of primary phase in the alloy is schematically presented as shown in Fig. 2. The initial amorphous phase is the chemically uniform amorphous solid solution and the primary phase of the Cu-free glassy alloy is Fe_{23}B_6 phase. As the amount of Cu goes up, the concentration of Cu in the clusters increases, and their structure becomes more like fcc. Because Cu has a large positive heat of mixing with respect to Fe [15], Fe atoms are rejected from Cu clusters and would pileup at the Cu/amorphous interface [18]. Then heterogeneous nucleation at the Cu/amorphous interface would be chemically more favorable than homogeneous nucleation inside the amorphous phase. The heterogeneous

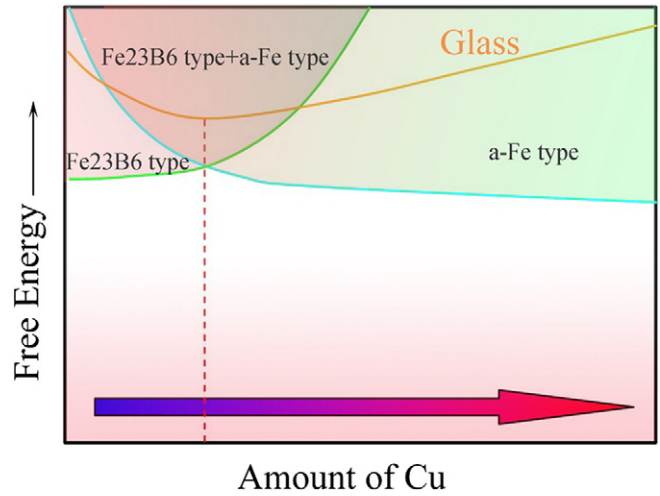


Fig. 2. The free energy diagram for $\text{Fe}_{72-x}\text{B}_{19.2}\text{Si}_{4.8}\text{Nb}_4\text{Cu}_x$ alloys.

nucleating potential barrier is smaller than homogeneous nucleating potential barrier [19]. Meanwhile, the Cu particle in amorphous alloys has the nearest neighbor structure similar to the fcc-Cu. The fcc-Cu (111) and bcc α -Fe (110) have very good matching [20]. Therefore, α -Fe (110) will be nucleated on the fcc-Cu (111) surface which can provide a low interfacial energy, i.e., Cu substitution can facilitate the segregation of α -Fe (110) phases. In addition, the Fe_{23}B_6 phase has a complex face-centered cubic structure with a large lattice parameter of more than 1 nm including 96 atoms [21], and its precipitation from the network-like glassy structure requires high energy and long-range atomic rearrangements of constituent elements. The competitive formation of the Fe_{23}B_6 and α -Fe (110) leads to the glassy phase upon the devitrification is drastically impeded. In consequence, the formation

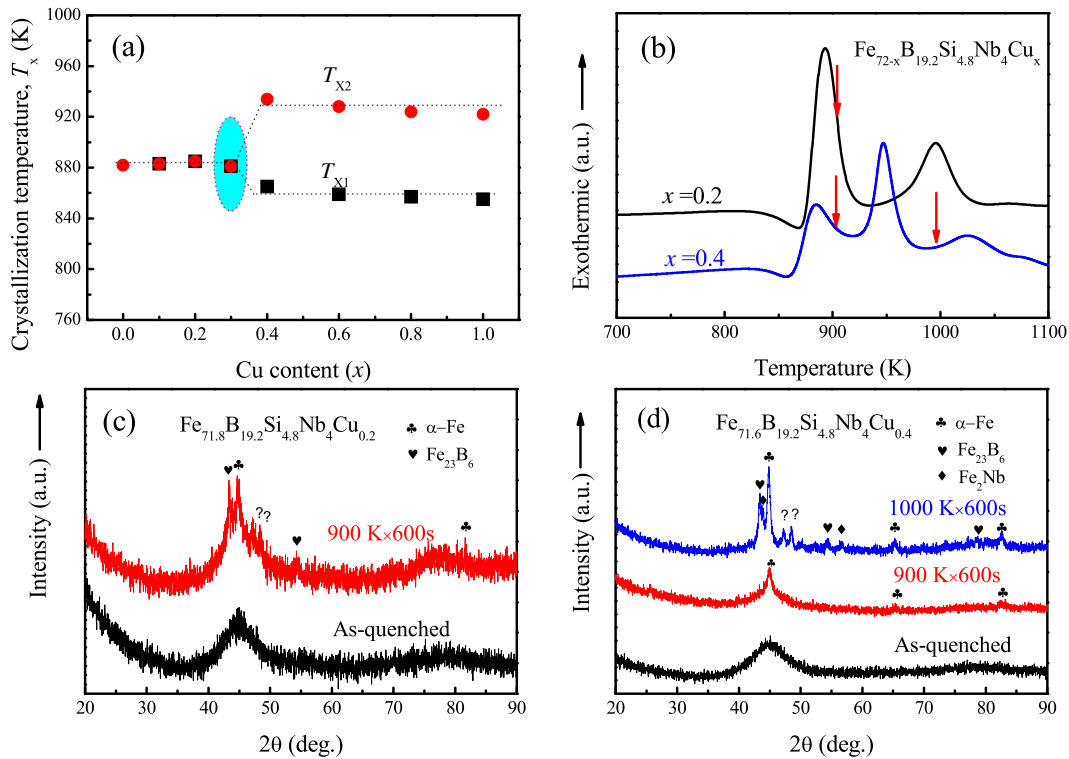


Fig. 1. Effects of Cu on the crystallization behavior in $\text{Fe}_{72-x}\text{B}_{19.2}\text{Si}_{4.8}\text{Nb}_4\text{Cu}_x$ ($x = 0, 0.1, 0.2, 0.3, 0.4, 0.6, 0.8, 1.0$) alloys. (a) Onset temperatures for crystallization, T_x , vs. Cu content. (b) DSC curves of the melt-spun $\text{Fe}_{71.8}\text{B}_{19.2}\text{Si}_{4.8}\text{Nb}_4\text{Cu}_{0.2}$ and $\text{Fe}_{71.6}\text{B}_{19.2}\text{Si}_{4.8}\text{Nb}_4\text{Cu}_{0.4}$ amorphous ribbons. (c) XRD patterns of the melt-spun $\text{Fe}_{71.8}\text{B}_{19.2}\text{Si}_{4.8}\text{Nb}_4\text{Cu}_{0.2}$ samples as quenched and annealed for 600 s at 900 K. (d) XRD patterns of the melt-spun $\text{Fe}_{71.6}\text{B}_{19.2}\text{Si}_{4.8}\text{Nb}_4\text{Cu}_{0.4}$ samples as quenched, annealed for 600 s at 900 K and 1000 K.

of competing crystalline phases is beneficial for the GFA [22] and the devitrification of $\text{Fe}_{71.7}\text{B}_{19.2}\text{Si}_{4.8}\text{Nb}_4\text{Cu}_{0.3}$ alloy will possess a higher GFA.

In order to confirm the above analysis, we check the maximum attainable diameter for glass formation as a function of the Cu contents and the corresponding XRD patterns for the as-cast rods, as shown in Fig. 3. It clearly demonstrates that GFA of the alloys is sensitive to the Cu content. As shown in Fig. 1, doping 0.3 at.% Cu in the alloy $\text{Fe}_{71.7}\text{B}_{19.2}\text{Si}_{4.8}\text{Nb}_4\text{Cu}_{0.3}$ apparently improves the GFA so the critical diameter is increased from 1.5 mm to 2.0 mm. However, excessive Cu doping (e.g., 0.8 at.%) reduces the GFA, which is consistent with above prediction. Furthermore, we also check the effects of Cu substitution on the crystallization behavior in $\text{Fe}_{72-x}\text{B}_{19.2}\text{Si}_{4.8}\text{Nb}_4\text{Cu}_x$ ($x = 0.1, 0.3$, and 0.8) alloys in the solidification processes. Fig. 4 shows the XRD patterns of the $\text{Fe}_{72-x}\text{B}_{19.2}\text{Si}_{4.8}\text{Nb}_4\text{Cu}_x$ rods ($x = 0.1, 0.3$ and 0.8) with different diameters. It is found that the primary phase of the Cu-free glassy alloy is Fe_{23}B_6 phase. However, the primary phase changed into α -Fe phase by further increasing Cu content above $x = 0.3$. Although the first crystallization peak was the same for $\text{Fe}_{72-x}\text{B}_{19.2}\text{Si}_{4.8}\text{Nb}_4\text{Cu}_x$ rods ($x = 0.3, 0.4, 0.6$ and 0.8), the refined α -Fe grains are more easily obtained for $\text{Fe}_{71.2}\text{B}_{19.2}\text{Si}_{4.8}\text{Nb}_4\text{Cu}_{0.8}$ alloy.

From the above analysis, we can conclude that minor substitution Cu in content (< 1 at.%) can substantially change the GFA of Fe-based amorphous alloys with the primary phase that is not α -Fe (110) phase. It has been reported that the high iron content alloys $\text{Fe}_{84}\text{Nb}_2\text{B}_{14}$ [23] and $\text{Fe}_{86}\text{B}_7\text{C}_7$ [24] exhibit high saturation magnetization, but a rather poor GFA, which limited their applications unfortunately. The primary phases

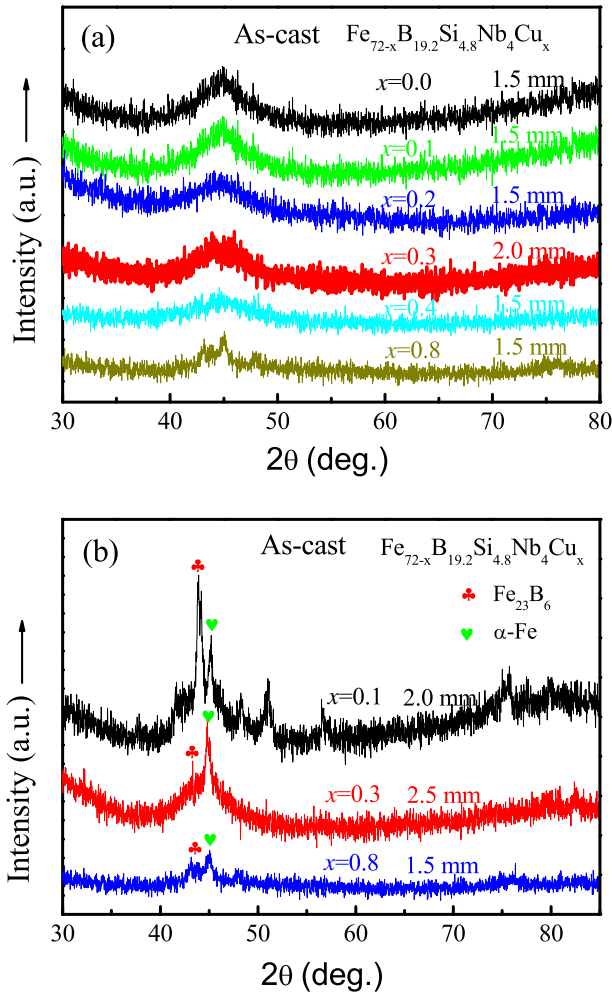


Fig. 3. (a) XRD patterns of the as-cast rods with the maximum diameters for the $\text{Fe}_{72-x}\text{B}_{19.2}\text{Si}_{4.8}\text{Nb}_4\text{Cu}_x$ ($x = 0, 0.1, 0.2, 0.3, 0.4, 0.8$) alloys. (b) XRD patterns of the $\text{Fe}_{72-x}\text{B}_{19.2}\text{Si}_{4.8}\text{Nb}_4\text{Cu}_x$ rods ($x = 0.1, 0.3$ and 0.8) with different diameters.

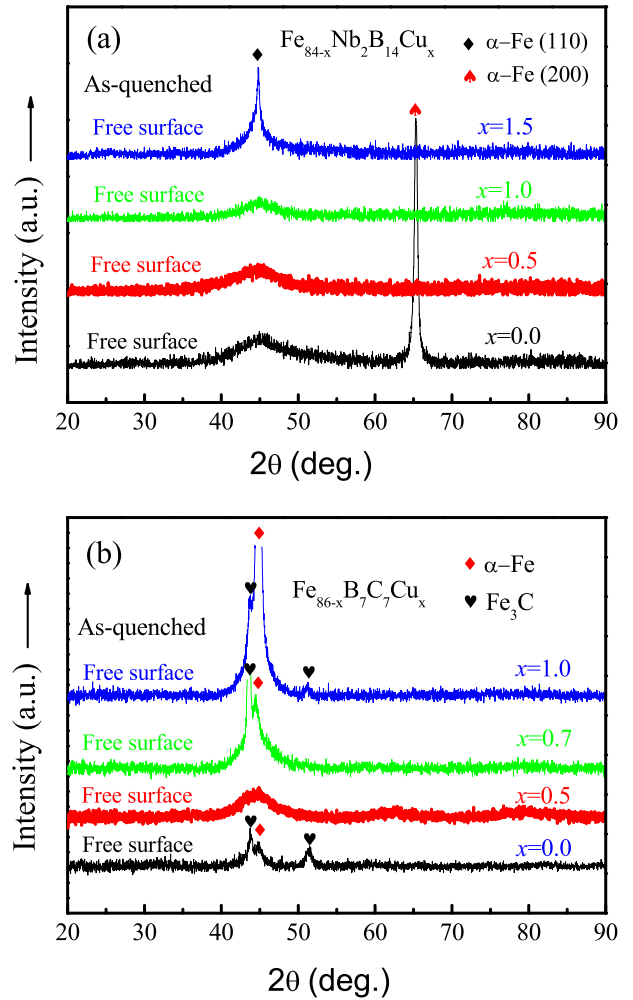


Fig. 4. (a) XRD patterns of as-quenched $\text{Fe}_{84-x}\text{Nb}_2\text{B}_{14}\text{Cu}_x$ alloys ($x = 0.0, 0.5, 1.0$ and 1.5). (b) XRD patterns of as-quenched $\text{Fe}_{86-x}\text{B}_7\text{C}_7\text{Cu}_x$ alloys ($x = 0.0, 0.5, 0.7$ and 1.0).

for these two alloys are determined as α -Fe (200) and Fe_3C , respectively. Here, we expect to enhance their GFA by doping minor substitution Cu using the above strategy. Fig. 4(a) and (b) shows the XRD patterns of as-quenched $\text{Fe}_{84-x}\text{Nb}_2\text{B}_{14}\text{Cu}_x$ ($x = 0.0, 0.5, 1.0$ and 1.5) and $\text{Fe}_{86-x}\text{B}_7\text{C}_7\text{Cu}_x$ ($x = 0.0, 0.5, 0.7$ and 1.0) alloys, respectively. As shown in Fig. 4(a), $\text{Fe}_{84-x}\text{Nb}_2\text{B}_{14}\text{Cu}_x$ specimens without Cu substitution show the sharp crystalline peaks on the main diffraction maximum, suggesting that the samples are partially amorphous with some crystalline phases. However, there are no discernible crystalline peaks on the XRD patterns of the as-quenched $\text{Fe}_{83.5}\text{Nb}_2\text{B}_{14}\text{Cu}_{0.5}$ and $\text{Fe}_{83}\text{Nb}_2\text{B}_{14}\text{Cu}_1$ samples with $\sim 25 \mu\text{m}$ thickness, suggesting that the alloy with 0.5 and 1.0 at.% Cu substitution is amorphous (within the limits of XRD resolution—some scarce dispersed nanocrystals cannot be fully excluded). Further increasing the Cu content to $x = 1.5$ leads to the crystalline peaks corresponding to α -Fe phase on the main halo, indicating that the sample consists of both amorphous and crystalline phases. These results indicate that the new alloys with 0.5 and 1.0 at.% Cu substitution have much better GFA than the original $\text{Fe}_{84}\text{Nb}_2\text{B}_{14}$ base alloy. Similarly, it also can be seen from Fig. 4(b) that the $\text{Fe}_{86-x}\text{B}_7\text{C}_7\text{Cu}_x$ specimens without Cu substitution show a number of sharp crystalline peaks on the main diffraction maximum, suggesting that the samples are partially amorphous with some crystalline phases. In contrast, there are no discernible crystalline peaks on the XRD pattern of the as-quenched $\text{Fe}_{85.5}\text{B}_7\text{C}_7\text{Cu}_{0.5}$ samples with $\sim 25 \mu\text{m}$ thickness, suggesting that the alloy with 0.5 at.% Cu substitution is amorphous. Further increasing the Cu content from $x = 0.7$ to $x = 1.0$ also leads to a number of

Table 1
Summary of the data on some Fe-based amorphous alloys.

Primary compositions	Critical amorphous thickness	Primary crystallization phase	Optimal amount of added elements (at.%)	Critical thickness	References
Fe ₇₂ B _{19.2} Si _{4.8} Nb ₄	1.5 mm	Fe ₂₃ B ₆	0.3	2 mm	This work
Fe ₈₄ Nb ₇ B ₁₄	<15 μm	α-Fe (200)	0.5	25 μm	This work
Fe ₈₆ B ₇ C ₇	<15 μm	Fe ₃ C	0.5	20 μm	This work
Fe ₈₄ P ₁₀ C ₆	<15 μm	Fe ₃ P	0.5	25 μm	[25]
Fe ₇₆ C ₇ Si _{3.3} B ₅ P _{8.7}	1.0 mm	Fe ₂₃ (C,B) ₆	0.3	3 mm	[26,27]
Fe ₇₆ Si ₉ B ₁₀ P ₆	2.5 mm	Fe ₂₃ B ₆	0.2	2.5–3.0 mm	[28]
Fe _{76.5} C ₆ S _{3.3} B _{5.5} P _{8.7}	1.0 mm	Fe ₂₃ B ₆	0.5	2.0 mm	[29]

crystalline peaks corresponding to α-Fe and Fe₃C phases superimposed on the main halo, indicating that the sample consists of both amorphous and crystalline phases. These results, therefore, demonstrate that the new alloy with 0.5 at.% Cu substitution has a much better GFA than the base alloy, which is consistent with above prediction.

Moreover, we further revisited the literatures about the enhanced GFA by tuning the glass compositions to check whether this concept also works for other Fe-based amorphous systems. Table 1 lists some typical Fe-based amorphous alloys and their improved GFA by minor Cu substitution. It can be found that the substitution of minor Cu by the main constituent Fe in different alloys also improves the GFA. Most importantly, the GFA improved alloys still possess a high iron content, confirming that the Fe-based amorphous alloys with good GFA and high saturation magnetization concurrently could be designed by slight tuning the Cu content.

4. Conclusions

In this paper, the enhanced GFA of high iron content amorphous alloys can be attributed to the minor substitution of Cu according to the formation of competing crystalline phases. Thereby, Fe-based amorphous alloys with high iron content and good GFA can be developed by this strategy. This work can provide guidance to design new Fe-based BMGs with high saturation magnetization and large GFA concurrently.

Acknowledgments

This work is supported by the Fundamental Research Funds for the Central Universities (2015QNA56).

References

- [1] J.E. Gao, Z.P. Chen, Q. Du, H.X. Li, Y. Wu, H. Wang, X.J. Liu, Z.P. Lu, *Acta Mater.* 61 (2013) 3214–3223.
- [2] L. Xue, H. Liu, L. Dou, W. Yang, C. Chang, A. Inoue, X. Wang, R.-W. Li, B. Shen, *Mater. Des.* 56 (2014) 227–231.
- [3] K. Suzuki, A. Makino, A. Inoue, T. Masumoto, *J. Appl. Phys.* 70 (1991) 6232–6237.
- [4] A. Inoue, N. Nishiyama, *MRS Bull.* 32 (2007) 651–658.
- [5] C. Suryanarayana, A. Inoue, *Int. Mater. Rev.* 58 (2013) 131–166.
- [6] W. Yang, H. Liu, C. Dun, J. Li, Y. Zhao, B. Shen, *J. Non-Cryst. Solids* 361 (2013) 82–85.
- [7] J. Li, W. Yang, M. Zhang, G. Chen, B. Shen, *J. Non-Cryst. Solids* 365 (2013) 42–46.
- [8] Z. Lu, C. Liu, J. Thompson, W. Porter, *Phys. Rev. Lett.* 92 (2004) 245503.
- [9] A. Inoue, T. Zhang, A. Takeuchi, *Appl. Phys. Lett.* 71 (1997) 464–466.
- [10] J. Li, W. Yang, D. Estévez, G. Chen, W. Zhao, Q. Man, Y. Zhao, Z. Zhang, B. Shen, *Intermetallics* 46 (2014) 85–90.
- [11] J. Shen, Q.J. Chen, J.F. Sun, H.B. Fan, G. Wang, *Appl. Phys. Lett.* 86 (2005) 151907.
- [12] D.H. Kim, J.M. Park, D.H. Kim, W.T. Kim, *J. Mater. Res.* 22 (2007) 471–477.
- [13] V. Ponnambalam, S.J. Poon, G.J. Shiflet, *J. Mater. Res.* 19 (2004) 1320–1323.
- [14] B.L. Shen, C.T. Chang, A. Inoue, *Intermetallics* 15 (2007) 9–16.
- [15] A. Takeuchi, A. Inoue, *Mater. Trans.* 46 (2005) 2817–2829.
- [16] J.G. Speight, in: M. Graw-Hill (Ed.), London, 2005, pp. 1.151.
- [17] M. Imafuku, S. Sato, H. Koshiba, E. Matsubara, A. Inoue, *Scr. Mater.* 44 (2001) 2369–2372.
- [18] K. Hono, D. Ping, M. Ohnuma, H. Onodera, *Acta Mater.* 47 (1999) 997–1006.
- [19] D. Turnbull, *J. Appl. Phys.* 21 (1950) 1022–1028.
- [20] J. Ayers, V. Harris, J. Sprague, W. Elam, *Magnetics, IEEE Trans.* 29 (1993) 2664–2666.
- [21] J. Zhang, B. Shen, Z. Zhang, *J. Non-Cryst. Solids* 360 (2013) 31–35.
- [22] D. Ma, H. Tan, D. Wang, Y. Li, E. Ma, *Appl. Phys. Lett.* 86 (2005) 191906–191903.
- [23] Z. Stokłosa, J. Rasek, P. Kwapuliński, G. Haneczok, A. Chrobak, J. Lelątko, L. Pająk, *Phys. Status Solidi* 207 (2010) 452–456.
- [24] S. Hatta, T. Egami, C. Graham Jr., *Appl. Phys. Lett.* 34 (2008) 113–115.
- [25] Y. Jin, X. Fan, H. Men, X. Liu, B. Shen, *Sci. Chin. Technol. Sci.* 55 (2012) 3419–3424.
- [26] J.E. Gao, H.X. Li, Z.B. Jiao, Y. Wu, Y.H. Chen, T. Yu, Z.P. Lu, *Appl. Phys. Lett.* 99 (2011) 052504.
- [27] H.X. Li, J.E. Gao, Y. Wu, Z.B. Jiao, D. Ma, A.D. Stoica, X.L. Wang, Y. Ren, M.K. Miller, Z.P. Lu, *Sci. Rep.* 3 (2013) 1983.
- [28] X. Li, H. Kato, K. Yubuta, A. Makino, A. Inoue, *Mater. Sci. Eng. A* 527 (2010) 2598–2602.
- [29] H.Y. Jung, S. Yi, *J. Alloys Compd.* 561 (2013) 76–81.